This is the accepted manuscript made available via CHORUS. The article has been published as:

Distribution of Linearly Polarized Gluons and Elliptic Azimuthal Anisotropy in Deep Inelastic Scattering Dijet Production at High Energy

Adrian Dumitru, Tuomas Lappi, and Vladimir Skokov

The distribution of linearly polarized gluons and elliptic azimuthal anisotropy in DIS dijet production at high energy

Adrian Dumitru[*]

Department of Natural Sciences, Baruch College, CUNY,
17 Lexington Avenue, New York, NY 10010, USA and
The Graduate School and University Center, The City University of New York, 365 Fifth Avenue, New York, NY 10016, USA

Tuomas Lappi[†]

Department of Physics, P.O. Box 35, 40014 University of Jyväskylä, Finland and
Helsinki Institute of Physics, P.O. Box 64, 00014 University of Helsinki, Finland

Vladimir Skokov[‡]

Department of Physics, Western Michigan University, Kalamazoo, MI 49008, USA and
RIKEN/BNL Research Center, Brookhaven National Laboratory, Upton, NY 11973, USA

We determine the distribution of linearly polarized gluons of a dense target at small x by solving the B-JIMWLK rapidity evolution equations. From these solutions we estimate the amplitude of $\sim \cos 2\phi$ azimuthal asymmetries in DIS dijet production at high energies. We find sizeable long-range in rapidity azimuthal asymmetries with a magnitude in the range of $v_2 = \langle \cos 2\phi \rangle \sim 10\%$.

Transverse momentum dependent (TMD) factorization [1, 2] in deep inelastic scattering predicts a distribution for linearly polarized gluons in an unpolarized target [3, 4]. This is reflected in $\cos 2\phi$ asymmetries in dijet production [5, 6] and in other processes [7–9]. To date little is known about the magnitude of these functions in the small-x regime of high energies. In this paper we perform first estimates of these functions by solving the B-JIMWLK renormalization group equations [10–21]. Also, we use our solutions to analyze the magnitude of the resulting $\cos 2\phi$ asymmetry in dijet production [5, 22] at leading order. These could be tested at a future electron-ion collider (EIC) [23, 24], where the small-x effects discussed here can be enhanced by using a nuclear target.

Recent data for high multiplicity p+p [25, 26] and p+Pb [27–33] data at the LHC have revealed long-range (in rapidity) angular $\cos 2\phi$ "ridge" correlations in particle production high multiplicity events. The magnitude of these long range correlations is conventionally parametrized in terms of $v_2 \equiv \langle \cos 2\phi \rangle$. In fact, the azimuthal correlation in DIS dijet production at high energy originates also from the long-ranged eikonal interaction and so results in a similar experimental signature as the "ridge". To make this connection explicit we shall parametrize the azimuthal structure arising from the linearly polarized gluon distribution in terms of $v_2 = \langle \cos 2\phi \rangle$, and determine its dependence on the rapidity imbalance of the dijet.

At leading order the cross section for inclusive production of a dijet in γ^*-nucleus scattering is given by [5, 6]

$$E_1 E_2 \frac{d\sigma^{\gamma_T^* A \to q\bar{q}X}}{d^3 k_1 d^3 k_2 d^2 b} = \alpha_{em} e_q^2 \alpha_s \delta\left(x_{\gamma^*} - 1\right) z(1-z) \left(z^2 + (1-z)^2\right) \frac{\epsilon_f^4 + P_\perp^4}{(P_\perp^2 + \epsilon_f^2)^4}$$
$$\times \left[xG^{(1)}(x, q_\perp) - \frac{2\epsilon_f^2 P_\perp^2}{\epsilon_f^4 + P_\perp^4} \cos(2\phi) \, xh_\perp^{(1)}(x, q_\perp) \right] , \quad (1)$$

$$E_1 E_2 \frac{d\sigma^{\gamma_L^* A \to q\bar{q}X}}{d^3 k_1 d^3 k_2 d^2 b} = \alpha_{em} e_q^2 \alpha_s \delta\left(x_{\gamma^*} - 1\right) z^2(1-z)^2 \frac{8\epsilon_f^2 P_\perp^2}{(P_\perp^2 + \epsilon_f^2)^4}$$
$$\times \left[xG^{(1)}(x, q_\perp) + \cos(2\phi) \, xh_\perp^{(1)}(x, q_\perp) \right] . \quad (2)$$

Here,

$$\vec{P}_\perp = (1-z)\vec{k}_1 - z\vec{k}_2 \ , \quad \vec{q}_\perp = \vec{k}_1 + \vec{k}_2 \quad (3)$$

are the dijet transverse momentum scale $\vec{P}_\perp$ and the transverse momentum imbalance $\vec{q}_\perp$, respectively. The transverse momenta of the produced quark and antiquark are given by $\vec{k}_1$ and $\vec{k}_2$ and their respective light-cone momentum fractions are z and $1 - z$; the dijet in-
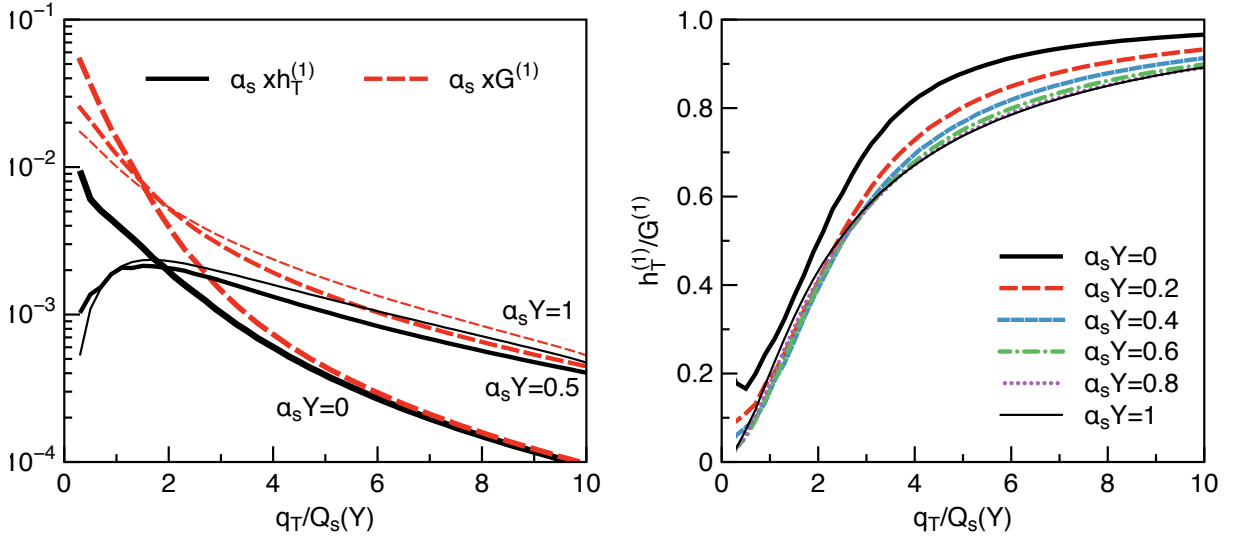
FIG. 1: Linearly polarized and unpolarized WW gluon distributions versus transverse momentum $q_\perp$ at different rapidities Y. Transverse momentum is measured in units of the saturation momentum $Q_s(Y)$. The curves correspond to evolution at fixed $\alpha_s = 0.15$.

variant mass is given by $M = P_\perp/\sqrt{z(1-z)}$. Also, $\epsilon_f^2 = z(1-z)Q^2$ with Q^2 of order $P_\perp^2$. Here, we restrict ourselves to kinematic configurations where $\vec{P}_\perp$ is greater than $\vec{q}_\perp$, referred to as the "correlation limit" in Refs. [5, 22].

In Eq. (2) ϕ denotes the azimuthal angle between $\vec{P}_\perp$ and $\vec{q}_\perp$, respectively. We introduce the following measure for the azimuthal anisotropy,

$$v_2 \equiv \langle \cos 2\phi \rangle \ . \tag{4}$$

The average over ϕ in this equation is performed with the weight (1) or (2), respectively. Since

$$x = \frac{1}{s}\left(q_\perp^2 + \frac{1}{z(1-z)}P_\perp^2\right) \tag{5}$$

is independent of ϕ, for a longitudinally/transversally polarized photon we have

$$v_2^L = \frac{1}{2}\frac{h_\perp^{(1)}(x, q_\perp)}{G^{(1)}(x, q_\perp)} \quad , \quad v_2^T = -\frac{\epsilon_f^2 P_\perp^2}{\epsilon_f^4 + P_\perp^4}\frac{h_\perp^{(1)}(x, q_\perp)}{G^{(1)}(x, q_\perp)} \ . \tag{6}$$

The linearly polarized $h_\perp^{(1)}$ and unpolarized $G^{(1)}$ distributions are defined as the traceless part and the trace of the Weizsäcker-Williams unintegrated gluon distribution, respectively:

$$xG_{\rm WW}^{ij} = \frac{1}{2}\delta^{ij}xG^{(1)} - \frac{1}{2}\left(\delta^{ij} - 2\frac{k^i k^j}{k^2}\right)xh_\perp^{(1)} \ . \tag{7}$$

In the CGC framework the gluonic degrees of freedom at small x are described by Wilson lines. They are path ordered exponentials in the strong color field of the target,

and cross sections for different observables can be related to different correlation functions of the Wilson lines. The Wilson line is a path ordered exponential of the covariant gauge field, whose largest component is A^+:

$$U(\mathbf{x}_T) = \mathbb{P}\exp\left\{ig\int dx^- A^+(x^-, \mathbf{x}_T)\right\} \ . \tag{8}$$

The Weizsäcker-Williams unintegrated gluon distribution [5, 22, 34], on the other hand, is expressed most naturally in terms of the light cone gauge ($A^+ = 0$) field, which has large transverse components. These can be obtained by a gauge transformation

$$A^i(\mathbf{x}_T) = \frac{1}{ig}U^\dagger(\mathbf{x}_T)\,\partial_i U(\mathbf{x}_T) \ . \tag{9}$$

Since, in light cone gauge, the gauge field lives above the light cone $A^i(\mathbf{x}_T, x^-) \sim \theta(x^-)A^i(\mathbf{x}_T)$, this field can also be thought of as a sheet of color electric field on the light cone $E^i(\mathbf{x}_T, x^-) = \delta(t-z)A^i(\mathbf{x}_T)$. The Weizsäcker-Williams distribution is simply the two-point correlator of the light cone gauge fields

$$xG_{\rm WW}^{ij}(x, \vec{k}) = \frac{8\pi}{L^2}\int \frac{d^2\mathbf{x}_T}{(2\pi)^2}\frac{d^2\mathbf{y}_T}{(2\pi)^2}e^{-i\mathbf{k}_T\cdot(\mathbf{x}_T-\mathbf{y}_T)}$$
$$\times \left\langle A_a^i(\mathbf{x}_T)A_a^j(\mathbf{y}_T)\right\rangle, \tag{10}$$

where we have normalized the distribution with the transverse area of the target L^2. This normalization drops out of the results expressed in terms of the elliptical asymmetry v_2. For analytical calculations of the functions $G^{(1)}(x_0, q_\perp)$ and $h_\perp^{(1)}(x_0, q_\perp)$ in the McLerran-Venugopalan (MV) model [35, 36], see Refs. [6, 22].
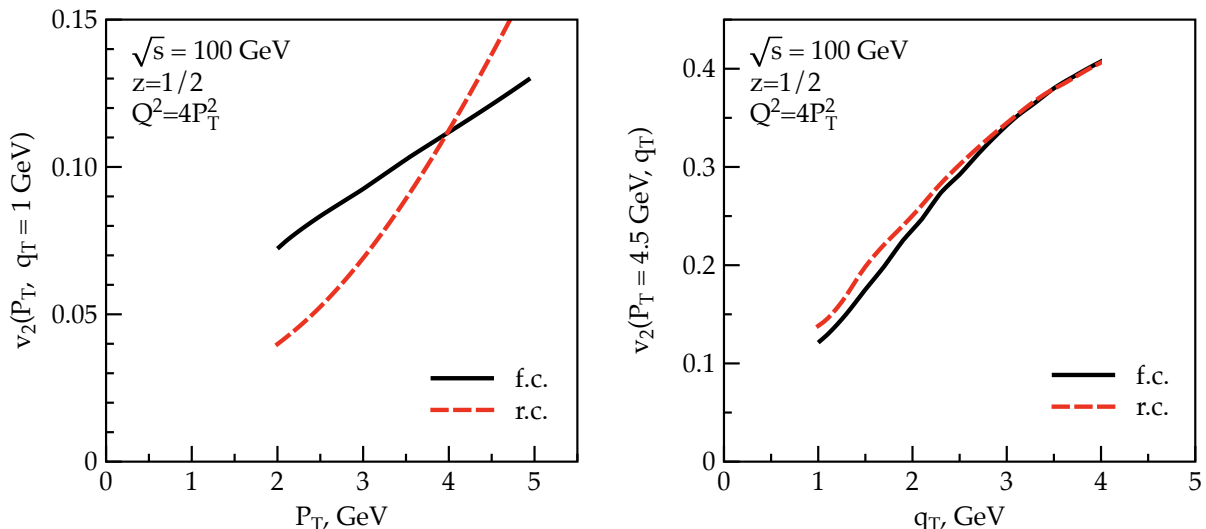
FIG. 2: The average azimuthal anisotropy $v_2 = \langle \cos 2\phi \rangle$ versus the dijet transverse momentum scale P_T or the dijet transverse momentum imbalance q_T, respectively. The assumed γ^*A center of mass energy is $\sqrt{s} = 100$ GeV. Since $Q^2 = 4P_\perp^2$ and $z = 1/2$ these curves apply to either longitudinal or transverse photon polarization. Solid (dashed) lines correspond to fixed (running) coupling evolution.

We obtain the Wilson lines U numerically from B-JIMWLK evolution in $Y = \ln(x_0/x)$, starting from an initial condition at $x_0 = 10^{-2}$ using the the MV model. The initial condition on the lattice is constructed as described in detail in Ref. [37]. The B-JIMWLK equation can be solved on the lattice with a Langevin method [38, 39]. We use here the "left-right" symmetric [40] numerical method introduced in Ref. [41], using either fixed coupling or a running coupling with the algorithm of Ref. [41]. As in e.g. Ref. [42], we determine the saturation scale Q_s numerically from the two-point (dipole) function of the Wilson lines. The renormalization group evolution increases Q_s roughly as $Q_s^2 \sim x^{-0.3}$. For the calculation of the light cone gauge field one needs Fourier transforms of derivatives of Wilson lines. Some care must be exercised to obtain the proper momentum space distribution: we have used two different centered difference methods (discretizing over one or two lattice spacings) and found that the results are equivalent. For the fixed coupling evolution we take $\alpha_s = 0.15$ to provide an evolution speed roughly in line with inclusive HERA data. For running coupling we use in this preliminary study the slightly overestimated value $Q_s(x_0)/\Lambda_{\mathrm{QCD}} = 11$, which also slows down the evolution closer to experimentally observed values.

For our numerical estimates below we take $Q^2 = 4P_\perp^2$. Hence, for $z = 1/2$, v_2^L and v_2^T have equal magnitude but there is a relative phase shift of $\pi/2$. The physical momentum scale is set by the saturation momentum at x_0. To obtain the numerical values in the plots we take $Q_s(x_0) = 1$ GeV (for a $q\bar{q}$ dipole). The saturation momentum corresponds to the scale where the forward

scattering amplitude is of order 1.

We now turn to describe our results. We first show the solution for the unintegrated gluon distributions before discussing the azimuthal asymmetry w.r.t. the direction of $\vec{q}_\perp$ of the γ^*A cross section.

Figure 1 shows the dependence of $G^{(1)}$ and $h_\perp^{(1)}$ at different evolution rapidities Y on transverse momentum. We refrain from showing curves for running coupling evolution since they look very similar. Either one of the TMDs drops rapidly as a power of $q_\perp$ at high transverse momentum $q_\perp \gg Q_s$ and so they are best measured at $q_\perp$ of order a few times the saturation scale. For a heavy-ion target the saturation scale is boosted (on average over impact parameters) by a factor of $\sim A^{1/3}$ [43] which facilitates such measurements in a regime of semi-hard $q_\perp$.

The degree of gluon linear polarization is maximal at high transverse momentum, $h_\perp^{(1)}/G^{(1)} \to 1$; the saturation of the positivity bound of the cross section has also been observed in perturbative twist-2 calculations of the small-x field of a fast quark [4, 6]. On the other hand $h_\perp^{(1)}/G^{(1)} \ll 1$ at low $q_\perp$ which conforms to the expected power suppression. At fixed $q_\perp/Q_s(x)$ the ratio of these functions decreases rather slowly with rapidity, at least after an initial evolution away from the MV model towards the B-JIMWLK fixed point. This means that, because of the growth of Q_s, the ratio $h_\perp^{(1)}/G^{(1)}$ at fixed transverse momentum $q_\perp$ decreases with rapidity. Thus the emission of additional small-x gluons reduces the degree of polarization. Our results show that this effect can quite well be parametrized by geometric scaling as a universal function of $q_\perp/Q_s$.
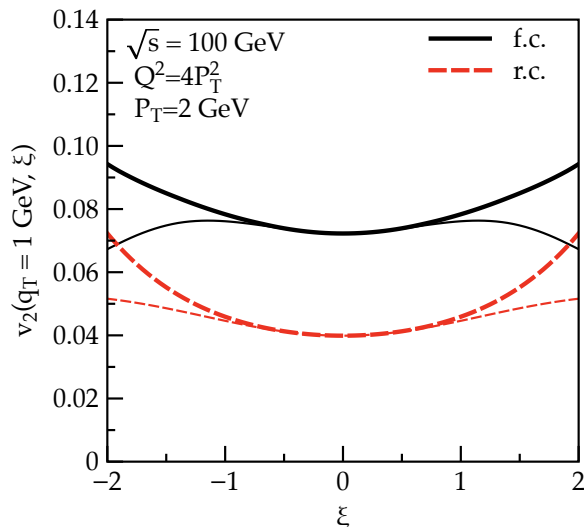
In Fig. 2 we show the elliptic asymmetry as a func-

FIG. 3: The average azimuthal anisotropy $v_2 = \langle \cos 2\phi \rangle$ versus the dijet rapidity imbalance $\xi = \log \ (1-z)/z$. Thick (thin) lines correspond to longitudinal (transverse) photon polarization.

tion of the dijet transverse momentum scale $P_\perp$ and the transverse momentum asymmetry $q_\perp$. Increasing $P_\perp$ increases x and suppresses evolution effects and so $v_2(P_\perp)$ increases towards the MV model initial condition. The reason for the difference between the fixed and running coupling curves in $v_2(P_\perp)$ is that in this preliminary study they have not been adjusted to have the same evolution speed $\partial_Y \ln Q_s^2(Y)$. We observe the same behavior for $v_2(q_\perp)$ even though x increases only slowly with $q_\perp$; here the increase of the elliptic asymmetry is mainly due to $h_\perp^{(1)}(q_\perp)/G^{(1)}(q_\perp) \to 1$ as $q_\perp/Q_s \gg 1$, as shown above. Overall, in the kinematic range considered in Fig. 2 we find a rather substantial magnitude of $v_2 \sim 10\%$.

Figure 3 shows v_2 versus the rapidity asymmetry

$$\xi = \log \frac{1-z}{z} \ . \tag{11}$$

Our calculation applies for moderately large rapidity separations less than $1/\alpha_s$, since we are assuming that the two jets are sensitive to the same distribution of Wilson lines. We find a mild increase of v_2 away from $z = 1/2$ which is due to the fact that asymmetric dijet configurations probe the gluon field of the target at larger values of x. The slow evolution of the eikonal interaction with x translates into a rather flat $v_2(\xi)$ over several units in ξ away from the boundary of phase space. Hence, at high energies the azimuthal asymmetry is long range in rapidity.

In summary, we have computed the TMD distribution $h_\perp^{(1)}$ of linearly polarized gluons for a large nucleus at small x. We have used the McLerran-Venugopalan model to obtain initial conditions at $x_0 \sim 10^{-2}$ and

the B-JIMWLK equations to evolve to lower x. We find that for realistic values of x and transverse momentum imbalance $q_\perp$ that $h_\perp^{(1)}(x, q_\perp)$ is of substantial magnitude. This results in large elliptic azimuthal asymmetries $v_2 \equiv \langle \cos 2\phi \rangle \sim 10\%$ in DIS dijet production. Also, the azimuthal correlations are long range in rapidity, i.e. v_2 depends weakly on the rapidity asymmetry $\xi = \log \ (1-z)/z$.

In the future we intend to check other initial conditions for the evolution, although we do not expect qualitative modifications of the results presented here. It will be interesting, also, to study Sudakov resummation effects [44, 45] as well as more general kinematic configurations which require quadrupole matrix elements [5].

* Electronic address: Adrian.Dumitru@baruch.cuny.edu
† Electronic address: Tuomas.v.v.Lappi@jyu.fi
‡ Electronic address: VSkokov@bnl.gov

[1] J. C. Collins and D. E. Soper, Nucl. Phys. **B194**, 445 (1982).
[2] R. Angeles-Martinez *et al.*, arXiv:1507.05267 [hep-ph].
[3] P. J. Mulders and J. Rodrigues, Phys. Rev. **D63**, 094021 (2001), [arXiv:hep-ph/0009343 [hep-ph]].
[4] S. Meissner, A. Metz and K. Goeke, Phys. Rev. **D76**, 034002 (2007), [arXiv:hep-ph/0703176 [HEP-PH]].
[5] F. Dominguez, C. Marquet, B.-W. Xiao and F. Yuan, Phys. Rev. **D83**, 105005 (2011), [arXiv:1101.0715 [hep-ph]].
[6] A. Metz and J. Zhou, Phys. Rev. **D84**, 051503 (2011), [arXiv:1105.1991 [hep-ph]].
[7] D. Boer, P. J. Mulders and C. Pisano, Phys. Rev. **D80**, 094017 (2009), [arXiv:0909.4652 [hep-ph]].
[8] D. Boer, S. J. Brodsky, P. J. Mulders and C. Pisano, Phys. Rev. Lett. **106**, 132001 (2011), [arXiv:1011.4225 [hep-ph]].
[9] J.-W. Qiu, M. Schlegel and W. Vogelsang, Phys. Rev. Lett. **107**, 062001 (2011), [arXiv:1103.3861 [hep-ph]].
[10] I. Balitsky, Nucl. Phys. **B463**, 99 (1996), [arXiv:hep-ph/9509348].
[11] I. Balitsky, Phys. Rev. Lett. **81**, 2024 (1998), [arXiv:hep-ph/9807434].
[12] I. Balitsky, Phys. Rev. **D60**, 014020 (1999), [arXiv:hep-ph/9812311].
[13] J. Jalilian-Marian, A. Kovner, A. Leonidov and H. Weigert, Nucl. Phys. **B504**, 415 (1997), [arXiv:hep-

ph/9701284].

[14] J. Jalilian-Marian, A. Kovner, A. Leonidov and H. Weigert, Phys. Rev. **D59**, 014014 (1999), [arXiv:hep-ph/9706377].

[15] J. Jalilian-Marian, A. Kovner and H. Weigert, Phys. Rev. **D59**, 014015 (1999), [arXiv:hep-ph/9709432].

[16] A. Kovner and J. G. Milhano, Phys. Rev. **D61**, 014012 (2000), [arXiv:hep-ph/9904420 [hep-ph]].

[17] A. Kovner, J. G. Milhano and H. Weigert, Phys. Rev. **D62**, 114005 (2000), [arXiv:hep-ph/0004014].

[18] E. Iancu, A. Leonidov and L. D. McLerran, Nucl. Phys. **A692**, 583 (2001), [arXiv:hep-ph/0011241].

[19] E. Iancu, A. Leonidov and L. D. McLerran, Phys. Lett. **B510**, 133 (2001), [arXiv:hep-ph/0102009].

[20] E. Ferreiro, E. Iancu, A. Leonidov and L. McLerran, Nucl. Phys. **A703**, 489 (2002), [arXiv:hep-ph/0109115].

[21] H. Weigert, Nucl. Phys. **A703**, 823 (2002), [arXiv:hep-ph/0004044 [hep-ph]].

[22] F. Dominguez, J.-W. Qiu, B.-W. Xiao and F. Yuan, Phys. Rev. **D85**, 045003 (2012), [arXiv:1109.6293 [hep-ph]].

[23] D. Boer *et al.*, arXiv:1108.1713 [nucl-th].

[24] A. Accardi *et al.*, arXiv:1212.1701 [nucl-ex].

[25] CMS, V. Khachatryan *et al.*, JHEP **1009**, 091 (2010), [arXiv:1009.4122 [hep-ex]].

[26] ATLAS, Measurement of two-particle correlations in $\sqrt{s} = 13$ TeV proton-proton collisions at the LHC with the ATLAS detector, ATLAS-CONF-2015-027.

[27] CMS, S. Chatrchyan *et al.*, Phys. Lett. **B718**, 795 (2013), [arXiv:1210.5482 [nucl-ex]].

[28] CMS, S. Chatrchyan *et al.*, Phys. Lett. **B724**, 213 (2013), [arXiv:1305.0609 [nucl-ex]].

[29] CMS, V. Khachatryan *et al.*, Phys. Rev. Lett. **115**, 012301 (2015), [arXiv:1502.05382 [nucl-ex]].

[30] ALICE, B. Abelev *et al.*, Phys. Lett. **B719**, 29 (2013), [arXiv:1212.2001 [nucl-ex]].

[31] ALICE, B. B. Abelev *et al.*, Phys. Rev. **C90**, 054901 (2014), [arXiv:1406.2474 [nucl-ex]].

[32] ATLAS, G. Aad *et al.*, Phys. Rev. **C90**, 044906 (2014), [arXiv:1409.1792 [hep-ex]].

[33] ATLAS, G. Aad *et al.*, Phys. Lett. **B725**, 60 (2013), [arXiv:1303.2084 [hep-ex]].

[34] D. Kharzeev, Y. V. Kovchegov and K. Tuchin, Phys. Rev. **D68**, 094013 (2003), [arXiv:hep-ph/0307037].

[35] L. D. McLerran and R. Venugopalan, Phys. Rev. **D49**, 2233 (1994), [arXiv:hep-ph/9309289].

[36] L. D. McLerran and R. Venugopalan, Phys. Rev. **D49**, 3352 (1994), [arXiv:hep-ph/9311205].

[37] T. Lappi, Eur. Phys. J. **C55**, 285 (2008), [arXiv:0711.3039 [hep-ph]].

[38] J.-P. Blaizot, E. Iancu and H. Weigert, Nucl. Phys. **A713**, 441 (2003), [arXiv:hep-ph/0206279 [hep-ph]].

[39] K. Rummukainen and H. Weigert, Nucl. Phys. **A739**, 183 (2004), [arXiv:hep-ph/0309306 [hep-ph]].

[40] A. Kovner and M. Lublinsky, JHEP **0503**, 001 (2005), [arXiv:hep-ph/0502071 [hep-ph]].

[41] T. Lappi and H. Mäntysaari, Eur. Phys. J. **C73**, 2307 (2013), [arXiv:1212.4825 [hep-ph]].

[42] A. Dumitru, T. Lappi and Y. Nara, Phys. Lett. **B734**, 7 (2014), [arXiv:1401.4124 [hep-ph]].

[43] H. Kowalski, T. Lappi and R. Venugopalan, Phys. Rev. Lett. **100**, 022303 (2008), [arXiv:0705.3047 [hep-ph]].

[44] L. Zheng, E. C. Aschenauer, J. H. Lee and B.-W. Xiao, Phys. Rev. **D89**, 074037 (2014), [arXiv:1403.2413 [hep-ph]].

[45] A. H. Mueller, B.-W. Xiao and F. Yuan, Phys. Rev. **D88**, 114010 (2013), [arXiv:1308.2993 [hep-ph]].